Understanding the Torsional Response of Unbonded Fiber Reinforced Elastomeric Isolators: A Finite Element Study

P. Ambili, S. C. Mohan, and S. Sistla

Abstract Conventional steel reinforced elastomeric isolators (SREI) have been widely used to improve the seismic performance of buildings; however, they are not economical for low-rise residential buildings in developing countries like India. Hence, Unbonded Fiber Reinforced Elastomeric Isolators (UFREI) have been developed as a cost-effective alternative to conventional isolators. Although studies have been conducted to understand the seismic behavior of UFREIs, limited research related to their torsional behavior was reported in the literature. Therefore, the primary aim of this study is to understand the torsional response of UFREIs by conducting finite element simulations on experimentally validated numerical models, using ABAQUS software. The rotational hysteresis behavior of UFREI with respect to the torsional moment and rotation is obtained and a detailed comparison of torsional stiffness with the increasing rotation is presented. These results are used to develop a two-storeyed base isolated RC framed building model in SAP 2000 software. The global torsional response of the building model is studied by conducting linear time history analyses using bi-directional ground motions. A comparative analysis of the behavior of the structure isolated by UFREI and the corresponding behavior of the traditional fixed base structure are presented to understand how the rotational response of UFREI influences the performance of building under earthquakes in both horizontal directions. The results show that the torsional behavior of isolator has negligible effect on the torsional response of the building under bi-directional ground motions.

P. Ambili (✉) · S. C. Mohan
Department of Civil Engineering, BITS Pilani, Hyderabad, India
e-mail: p20210437@hyderabad.bits-pilani.ac.in

S. C. Mohan
e-mail: mohansc@hyderabad.bits-pilani.ac.in

S. Sistla
Department of Civil and Natural Resources Engineering, University of Canterbury, Christchurch, New Zealand
e-mail: ssi178@uclive.ac.nz

M. Shrikhande et al. (eds.), *Proceedings of 17th Symposium on Earthquake Engineering (Vol. 1)*, Lecture Notes in Civil Engineering 329,
https://doi.org/10.1007/978-981-99-1608-5_33

Keywords Unbonded fiber reinforced elastomeric isolators · Finite element simulations · Linear time history analyses · Bi-directional ground motions

1 Introduction

Significant earthquakes in the past have demonstrated the necessity for seismic-resistant design of new structures and rehabilitation of existing facilities, due to the havoc caused by such events in terms of casualties and economic losses [1]. To meet the seismic-resistant design criteria, the structures should be provided with suitable seismic isolation systems or lateral load-resisting devices such as shear walls or braced frame systems. Unlike lateral load-resisting systems that increase the seismic capacity of structures, base isolators are passive earthquake-resistant systems that reduce the seismic demand on structures. Although there are many innovative advances in base isolation systems, elastomeric bearings and sliding isolators are the most widely used application. Studies reveal that Traditional Steel Fiber Reinforced Elastomeric Isolators (SREIs) can support sufficient loads and provide high levels of seismic isolation. However, these are extremely heavy and involve higher costs due to the usage of steel, installation and maintenance, making them unfeasible for residential purposes [2, 3].

In developing nations like India where the majority of buildings are low to mid-rise and the earthquake-induced damages are more severe due to inadequately designed, outdated structures, it is necessary to implement low-cost seismic protection measures without sacrificing their effectiveness. This low-cost requirement can be achieved by adopting Fiber Reinforced Elastomeric Isolators (FREIs) in which the steel layers (as in the case of SREIs) are replaced with appropriate fiber reinforcement that would provide sufficient vertical stiffness as well as horizontal flexibility, thereby isolating the structure from ground motions [3]. The fiber reinforcement consists of locally available fibers woven into fabrics interleaved between the rubber sheets. The weight and the cost of FREIs can be reduced considerably by removing the fixing plates bolted to the foundation and column of the structure. This method of application of FREI, known as the Unbounded Fiber Reinforced Elastomeric Isolator (UFREI), makes the installation simple and eliminates the need for bonding at contact surfaces, reducing the overall cost of production [4]. The large-scale production of bearings required for low-cost public housing in seismic-prone areas can be made possible by manufacturing longer strips of isolator and cutting them into necessary sizes [5].

In the case of Unbonded FREIs, the top and bottom end surfaces can undergo a roll-off phenomenon between the supports on increasing the horizontal displacements. Figure 1a shows the rollover deformation of UFREI under lateral loading. On full rollover (Fig. 1b), the bearing detaches from the supports and consequently, the lateral surfaces of the bearing rotate to touch the supporting horizontal plates [4]. The rollover deformation reduces the horizontal stiffness of the bearing, thus softening is observed with a reduction in the effective area of contact, which helps in shifting the

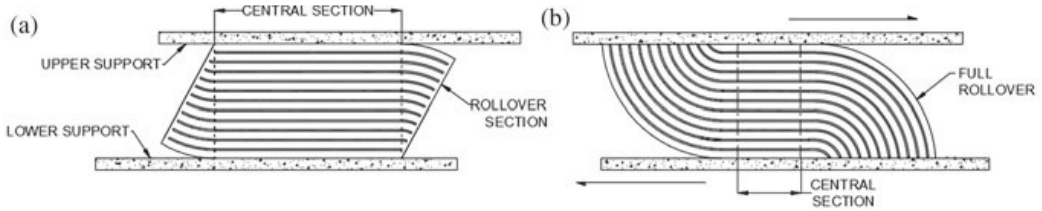

Fig. 1 **a** Rollover deformation of UFREI under horizontal displacements; **b** UFREI undergoing full rollover

time period of the structure during earthquakes. The stiffening of the isolator at full rollover acts like a safety mechanism against very high displacements [4]. Theoretical and experimental investigations done by Moon et al. [5] on strip-type carbon Fiber Reinforced Elastomeric Isolators. The results indicate that strip-type isolators behave similar to steel reinforced elastomeric isolators and are advantageous for retrofitting masonry structures [5]. Kelly and Calabrese [4] conducted an experimental investigation to assess the stiffness and damping characteristics of FREIs with various shapes, including circular, square and strip types [4]. They have introduced a simple design criterion for evaluating the vertical stiffness, maximum lateral displacement and tensile stresses in the fiber layers. Thuyet et al. [6] evaluated the effectiveness of UFREIs in controlling the seismic vulnerability of a masonry building in India using fragility curves and found that the base isolated building exhibited a lower risk of exceeding all the considered damage states than the fixed base building [6]. Pauletta [7] proposed a step-by-step methodology for the design of square-shaped UFREIs and applied it to a six storeyed building [7]. Habieb and Milani [8] evaluated the response of a masonry church using both bonded and unbounded FREIs and found that UFREIs are better in performance under moderate to severe earthquakes [8].

Teja and Mohan [9] carried out the parametric studies to understand the role of various fibers like jute, sisal, glass, flax, kevlar and carbon in the performance of FREIs and their applicability for base isolation in low-rise RC buildings [9]. They observed that flax fiber is better in terms of economy and performance.

Most of the experiments conducted on UFREIs are based on two degrees of freedom where the vertical load, as well as the horizontal displacements, is imposed. The behavior of UFREI in torsion is not sufficiently taken into account [10]. In reality, structures are subjected to two horizontal orthogonal components of ground motions. Though researches have been carried out to evaluate the performance of UFREIs, studies on their behavior under bi-directional ground motions are limited. So in this study, numerical analyses are carried out to investigate the torsional behavior of UFREIs adopted in low-rise RC framed buildings subjected to bi-directional ground motions.

2 Numerical Study

To evaluate the torsional response of UFREIs with locally available fibers under bi-directional loading, isolator properties as suggested from the parametric studies done by SaiTeja and Mohan [9] are adopted. The numerical model has been validated in a previous study by SaiTeja and Mohan [9]. Parameters such as vertical stiffness, horizontal stiffness and equivalent damping ratios of the isolator are determined considering the axial, lateral and torsional degrees of freedom, which are used as inputs for carrying out the time history analysis of the base isolated RC framed building.

2.1 Material Properties

In order to represent the rubber numerically, it is essential to evaluate its hyper-elastic and visco-elastic properties. Hyper-elasticity is the ability of the material to undergo large deformations without yielding while visco-elasticity is the ability of the material to show strain and time-dependent elastic and viscous properties leading to energy dissipation. These properties are represented with the help of Yeoh's hyper-elasticity model [11, 12] and Prony series coefficients [13] as shown in Tables 1 and 2.

From the parametric studies on UFREI conducted by SaiTeja and Mohan [9], involving gauging the effects of different locally available fiber materials on the performance of isolator, it was observed that flax fiber is economical and also has good performance in terms of vertical and horizontal stiffness as well as damping. The ultimate strength range of flax fiber is 600–800 N/mm^2 with a young's modulus and Poisson's ratio of 50,000 N/mm^2 and 0.23, respectively.

Table 1 Hyper-elastic properties of rubber

C_{10} (MPa)	C_{20} (MPa)	C_{30} (MPa)	D_1	D_2	D_3
0.2551	0.0066	0.000032	0.00218	8.68E–05	− 1.79E–05

Table 2 Visco-elastic properties of rubber

g	T
0.333	0.04
0.333	100

Table 3 Geometric and dynamic properties of UFREI

Description	Value
Shear modulus of rubber	0.42 MPa
Planar area of isolator	200 mm × 100 mm
Load on each isolator	6116 kg
Pressure on each isolator	3.0 N/mm^2
Total thickness of isolator (t_i)	60 mm
Number of fiber layers	8
Number of rubber layers	9
Thickness of one fiber layer	0.25 mm
Thickness of one rubber layer	6.45 mm

2.2 Geometric Properties

The dimensions of the isolator and its components are adopted based on the stiffness and time period requirements [9]. To achieve the best results, the time period of the isolator should be approximately three times that of the fundamental time period of the structure. The geometric properties of UFREI as suggested by SaiTeja and Mohan [9] along with its dynamic properties are given in Table 3.

2.3 Modeling and Numerical Simulation

The numerical simulation of UFREI reinforced with flax fiber is carried out using the finite element package, ABAQUS to obtain the stiffness and damping properties which is further used as input in SAP 2000 software. The model of UFREI is shown in Fig. 2. The red colored elements in the model represent mild steel plates, the black colored elements represent rubber and black colored elements represent fiber sandwiched between the rubber layers. To provide the unbonded condition in the bearing, a penalty function (friction coefficient = 0.85) is used to formulate the friction between the rubber layer and the surface of the supporting plates [14].

The isolator is subjected to 60 mm peak horizontal displacement with a corresponding amplitude factor as shown in Fig. 3. This peak displacement corresponds to 100% shear strain, hence, the peak displacement is taken as the thickness of isolator. Based on the time separation factor between 2 and 3, the expected natural frequency of the base isolated structure was around 1 Hz, hence the quasi-static test is carried out at 1 Hz in the present study. A constant vertical pressure of 3.0 N/mm^2 is applied on the top plate which corresponds to the load carried by a single isolator. A maximum rotation of 0.9667 radians corresponding to a shear strain of 150% is applied about the vertical axis of the isolator to evaluate its torsional behavior. The required rotation is calculated using the equation of torsion for rectangular sections undergoing twisting about their vertical axis [15]. The plan view of UFREI showing

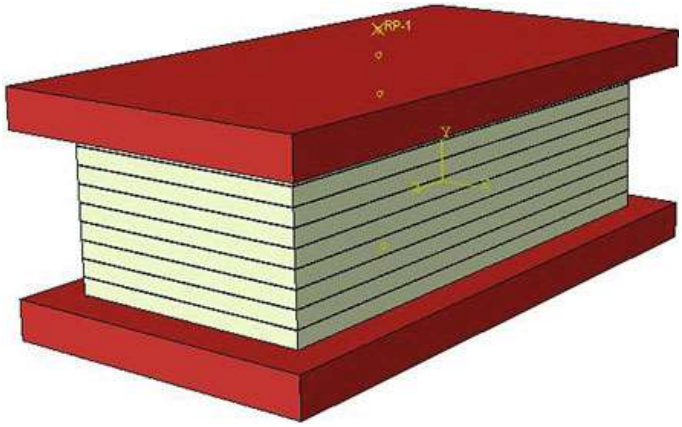

Fig. 2 UFREI model in ABAQUS

the geometric properties and undergoing rotation about the vertical axis are shown in Fig. 4.

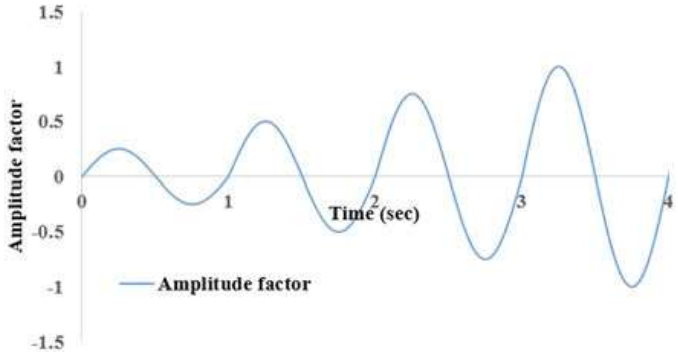

Fig. 3 Amplitude factor versus time graph

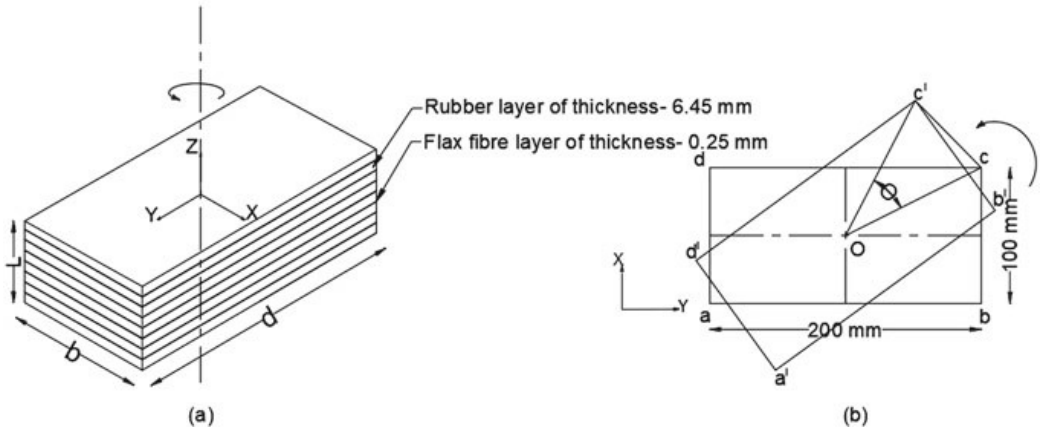

Fig. 4 Plan view of the bearing **a** showing geometric properties, and **b** undergoing rotation about the vertical axis

2.4 ABAQUS Simulation Results

The force–displacement curves are obtained for translational motion as well as torsion. As the horizontal displacement is increasing, the effective area of contact (bearing area) between the rubber and plate is decreasing and hence there is a reduction in stiffness of the isolator. The hysteresis is plotted for 4 different cycles, i.e., 25% of 60 mm, 50% of 60 mm, 75% of 60 mm and 100% of 60 mm as seen in Fig. 4. The characteristics of UFREI such as the horizontal stiffness and equivalent viscous damping ratio can be obtained from the final cycle of hysteresis loops using the following equations [3].

$$K_{\text{eff}}^{h} = \frac{F_{\max} - F_{\min}}{d_{\max} - d_{\min}} \tag{1}$$

$$\xi = \frac{W_d}{4\pi W_s} \tag{2}$$

$$W_s = \frac{K_{\text{eff}}^{h}(\Delta_{max})^2}{2} \tag{3}$$

$$\Delta_{\max} = \frac{d_{\max} - d_{\min}}{2} \tag{4}$$

where K_{eff}^{h} is the effective horizontal stiffness, $F_{\max}$, $F_{\min}$, $\Delta_{\max}$, $\Delta_{\min}$ are the maximum and minimum horizontal force and applied displacement, respectively, ξ represents the damping ratio, W_s is the energy stored and W_d is the energy dissipated. The calculated values of horizontal stiffness and corresponding damping ratios (ξ) are summarized in Table 4.

Horizontal Behavior

The hysteresis loops for the considered UFREI corresponding to the displacements applied in both horizontal directions are given in Fig. 5. As the dimension of UFREI is less along the X-direction, the increase in lateral displacement along this direction results in more rollover action of the isolator. This results in reduction of effective contact area of the isolator with the top and bottom surfaces which leads to a more non-linear shaped hysteresis loop as compared to the rollover effect occurring when

Table 4 Stiffness and damping properties of UFREI

Description	K value	ξ (%)
Horizontal stiffness (in X-direction), (K_{eff}^{x})	155.74 N/mm	10.15
Horizontal stiffness (in Y-direction), (K_{eff}^{y})	280.88 N/mm	6.99
Vertical stiffness, (K_{eff}^{v})	64,402.55 N/mm	
Torsional Stiffness (K_{Θ})	1,296,148.80 N-mm/rad	

the displacement is given along its longer dimension. Since the UFREI has a larger dimension in the y-direction, rollover action causes less reduction in the contact area. This results in not much reduction in the horizontal stiffness with displacement leading to a less non-linear hysteresis loop. Thus, the stiffness in the horizontal Y-direction is found to be larger than that of the X-direction.

Figures 6 and 7 shows the rollover action due to the lateral deformation of UFREI along the X and Y axes and the corresponding Von-Mises stress distributions. It can be observed from the graph that the stresses in fiber layers haven't exceeded their yield strength.

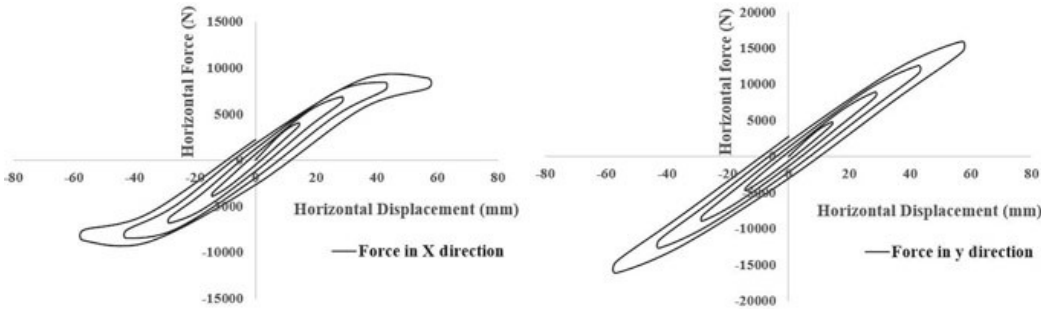

Fig. 5 Hysteresis plots for UFREI corresponding to displacements in X and Y axes

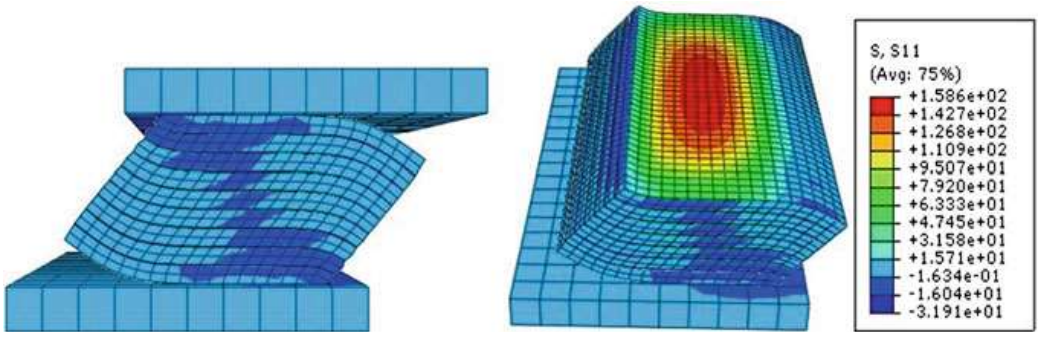

Fig. 6 Stress distribution corresponding to displacement in horizontal X-direction

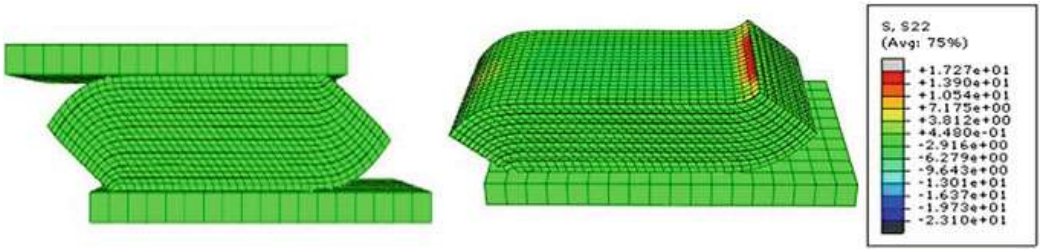

Fig. 7 Stress distribution corresponding to displacement in horizontal Y-direction

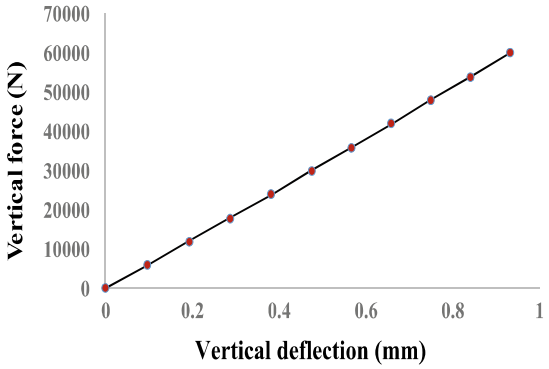

Fig. 8 Vertical load–displacement plot

Vertical behavior

The vertical stiffness of the bearing can be obtained from the force versus vertical displacement graph shown in Fig. 8, and the value obtained is given in Table 4. This vertical stiffness corresponds to the loading due to self-weight and live load on the structure.

Torsional behavior

Previously, many researchers have not considered the rotational behavior of the isolation systems since it does not have a significant difference in the analysis under uni-directional earthquake loading [16]. Habieb et al. have suggested equations to compute the rotational stiffness of the isolation system with some marginal error. The torsional moment vs rotation plot for the isolation system is shown in Fig. 9.

The isolator is subjected to a maximum rotation of 0.9667 radians about the vertical axis. The torsional stiffness of the UFREI is around 1,296,148.80 N-mm/rad. The stiffness is not very high and it may be due to the lift-off observed (Fig. 9) during the rotation of the isolator, that is the loss of contact at the ends between the UFREI and the supports resulting in the reduction in the loaded area of the bearing. Figure 10 shows the torsional deformation of the elastomeric bearing and the corresponding

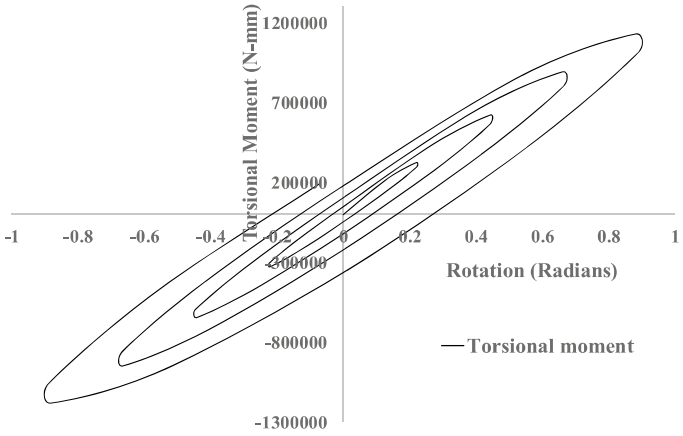

Fig. 9 Torsional hysteresis plots for UFREI

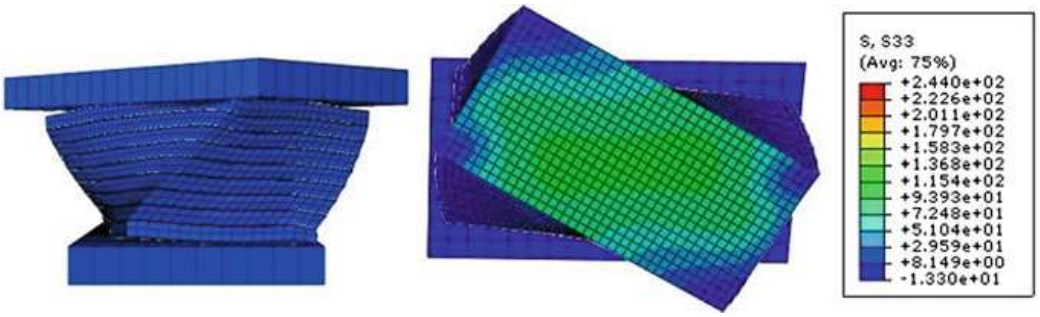

Fig. 10 Stress distribution corresponding to rotation about the vertical axis

Von-Mises stress distribution. It is seen that the stresses in the fiber have not exceeded the ultimate tensile strength.

3 Performance of Base Isolated Structure

For evaluating the response of the base isolated structure considering the bi-directional ground motions, the two uni-directional translational hysteresis models in each of the principal directions are used along with the torsional hysteresis. The vertical stiffness, horizontal stiffness as well as damping coefficients obtained from ABAQUS simulations were taken as inputs for assessing the performance of a two-storeyed isolated RC framed building in SAP 2000 v20.1.0 software. The hysteresis loop of UFREI is represented with the help of a multi-linear plastic link element in the software. The plan and details of the building considered are given in Fig. 11 and Table 5, respectively. Linear dynamic analysis of the building with isolated base and fixed base is carried out using seven different ground motions scaled to the target response spectrum of IS 1893 Part-1:2016 for zone V [17]. The software Seismomatch is used to match the selected earthquakes. The superstructure is assumed to be in the elastic range as less energy is transferred to the superstructure from the base during earthquakes whereas the isolation system is considered to be non-linear.

The roof displacement response obtained from the time history analysis for two ground motions–Chi Chi (1999) and Northridge (1994) are given in Figs. 12 and 13, respectively. It is seen that the top storey displacements of the fixed building have exceeded the allowable deflection (L/250) for most of the ground motions considered. As a result of increase in the time period, the isolated building shows an average reduction in the roof displacement along the X- and Y-directions by 83% and 79%, respectively, and the interstorey drift by 82% and 78%, respectively (Fig. 14). As a result of reduced roof accelerations, the storey shear for base isolated building is reduced by 52.2% along the X-direction and 40.1% along the Y-direction on an average compared to that of the fixed base building as shown in Fig. 15.

To understand the torsional behavior of building with and without isolation, the peak displacement at the stiff and flexible corners of the building are plotted as shown

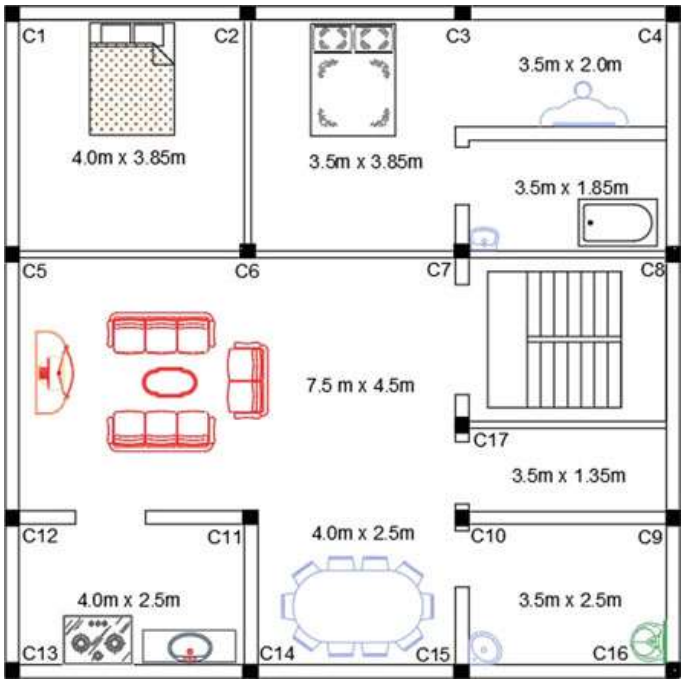

Fig. 11 Plan of two-storeyed RC framed building

Table 5 Building properties and loading details

Description	Value
Grade of concrete and steel	M20, Fe415
Beam size	240 mm × 240 mm
Column size	270 mm × 270 mm
Slab thickness	100 mm
Live load	2 kN/m^2
Floor finish	1 kN/m^2
Wall load	12.96 kN/m
Floor height	3 m
Number of columns	17
Seismic zone [India]	V
Soil type	Medium
Total mass of the structure (M)	110 tons
Fundamental time period of fixed building	0.45 s
Time period of isolated system	1.67 s

in Fig. 16. The eccentricity of the building considered is found to be 0.57% and in X-direction and 5.0% in Y-direction, which is very less. Both stiff and flexible side displacements are found to be similar with negligible variation. This shows that the effect of torsional behavior of UFREI is negligible for buildings with less eccentricity.

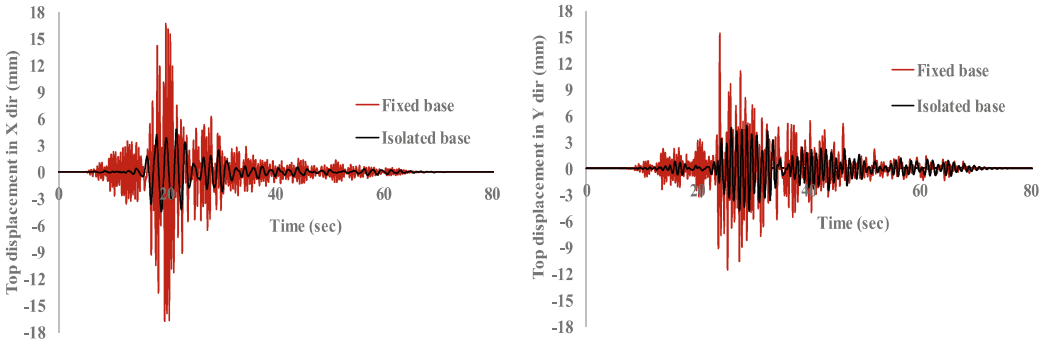

Fig. 12 Roof displacement responses along X- and Y-directions–Chi Chi earthquake

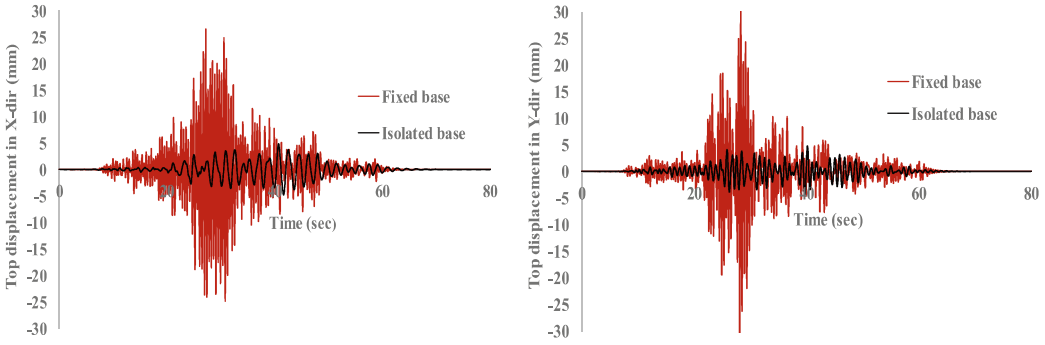

Fig. 13 Roof displacement responses along X- and Y-directions–Northridge earthquake

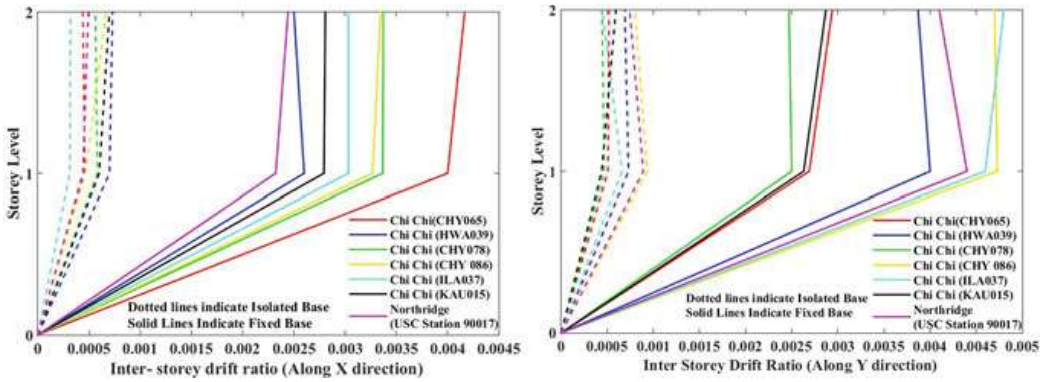

Fig. 14 Inter-storey drift ratios along X- and Y-directions

4 Conclusions

The paper presents the study on evaluating the torsional behavior of rectangular-shaped UFREIs when applied to low-rise buildings subjected to bi-directional ground motions. The numerical study is carried out using the software, ABAQUS. The vertical stiffness, effective stiffness along both the horizontal directions and the

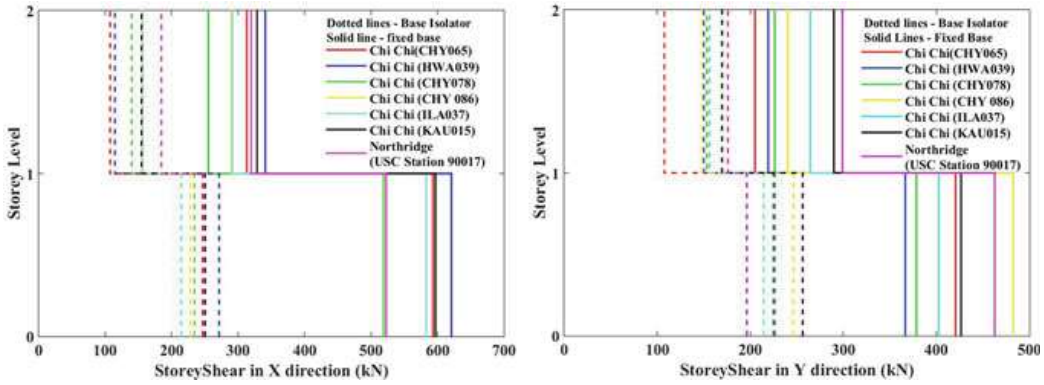

Fig. 15 Storey shear along X- and Y-directions

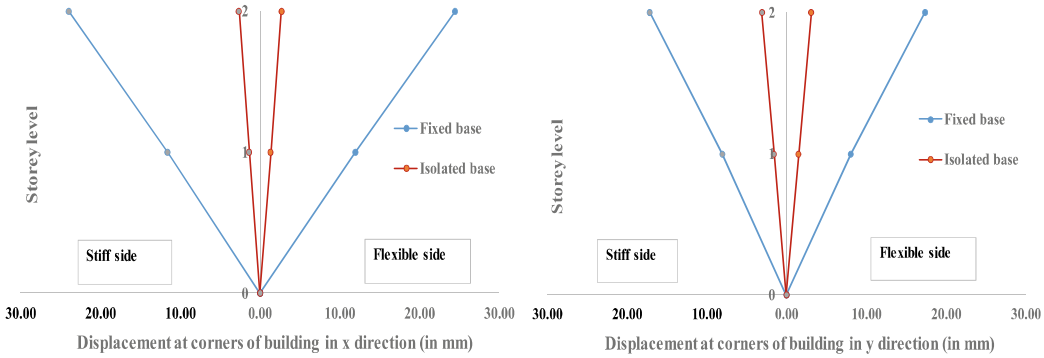

Fig. 16 Displacements at the stiff and flexible side of the building

torsional stiffness are determined. It is observed that the adopted UFREI has adequate torsional stiffness in addition to horizontal flexibility and vertical stiffness. The comparison of time history results of a two-storeyed RC building with fixed and isolated base subjected to bi-directional ground motions shows significant reduction in roof level displacements and the storey shear along both horizontal directions. From the observations, it is clear that the torsional behavior of UFREI has very little impact on the torsional response of the building with reduced eccentricity when subjected to bi-directional ground motions. Further studies can be carried out to evaluate the torsional behavior of irregular-shaped isolated buildings with large eccentricities.

References

1. Takagi, J., Wada, A.: Recent earthquakes and the need for a new philosophy for earthquake-resistant design. Soil Dyn. Earthq. Eng. **119**, 499–507 (2019)
2. Kelly, J.M.: Earthquake-Resistant Design with Rubber. Springer, London (1993)
3. Naeim, F., Kelly, J.M.: Design of Seismic Isolated Structures: From Theory to Practice. Earthq. Spectra. **16** (1999)

4. Kelly, J.M., Calabrese, A.: Mechanics of Fiber Reinforced Bearings (2012)
5. Moon, B.Y., Kang, G.J., Kang, B.S., Kim, G.S., Kelly, J.M.: Mechanical properties of seismic isolation system with fiber-reinforced bearing of strip type. Int. Appl. Mech. **39**, 1231–1239 (2003)
6. Thuyet, V.N., Deb, S.K., Dutta, A.: Mitigation of seismic vulnerability of prototype low-rise masonry building using U-FREIs. J. Perform. Constr. Facil. **32** (2018)
7. Pauletta, M.: Method to design fiber-reinforced elastomeric isolators (U-FREIs) and application. Eng. Struct. **197** (2019)
8. Habieb, A.B., Milani, G., Tavio, T.: Two-step advanced numerical approach for the design of low-cost unbonded fiber reinforced elastomeric seismic isolation systems in new masonry buildings. Eng. Fail. Anal. **90**, 380–396 (2018)
9. Sistla, S., Mohan, S.C.: Parametric studies and application of fibre reinforced elastomeric isolators to low-rise buildings. Structures **34**, 2679–2693 (2021)
10. Habieb, A.B., Valente, M., Milani, G.: Hybrid seismic base isolation of a historical masonry church using unbonded fiber reinforced elastomeric isolators and shape memory alloy wires. Eng. Struct. **196**, 109281 (2019)
11. Yeoh, O.H.: Some forms of the strain energy function for rubber (1993)
12. Shahzad, M., Kamran, A., Siddiqui, M.Z., Farhan, M.: Mechanical characterization and FE modelling of a hyperelastic material. Mater. Res. **18**, 918–924 (2015)
13. Yu, T., Yin, S., Quoc, T., Liu, C., Wattanasakulpong, N.: Buckling isogeometric analysis of functionally graded plates under combined thermal and mechanical loads. Compos. Struct. **162**, 54–69 (2017)
14. Habieb, A.B., Valente, M., Milani, G.: Base seismic isolation of a historical masonry church using fiber reinforced elastomeric isolators. Soil Dyn. Earthq. Eng. **120**, 127–145 (2019)
15. Timoshenko, Strength of materials, part1, elementary theory and problems
16. Habieb, A.B., Valente, M., Milani, G.: Implementation of a simple novel Abaqus user element to predict the behaviour of unbonded fiber reinforced elastomeric isolators in macro-scale computations. Bull. Earthq. Eng. **17**, 2741–2766 (2019)
17. IS 1893 (Part 1): IS 1893 (Criteria for Earthquake resistant design of structures,Part 1:General Provisions and buildings). Bur. Indian Stand. New Delhi. **1893**, 1–44 (2016)